
XWOD: A Real-World Benchmark for Object Detection under Extreme Weather Conditions

Chih-Hsin Chen, Yu-Tung Liu, Amar Fadillah, Kuan-Ting Lai
Department of Electronic Engineering
National Taipei University of Technology
{t111C71102, t113368501, t112999405, ktlai}@ntut.edu.tw

Dong Liu
Adobe Inc.
dongliu.hit@gmail.com

Abstract

Autonomous driving and intelligent transportation systems remain vulnerable under extreme weather. The U.S. Federal Highway Administration reports that roughly 745,000 crashes and 3,800 fatalities per year are weather-related, and recent regulatory investigations have examined failures of Level-2/3 driving systems under reduced-visibility conditions. However, datasets commonly used to evaluate weather robustness remain limited in scale, diversity, and realism. In this paper, we introduce XWOD (Extreme Weather Object Detection), a large-scale real-world traffic-object detection benchmark containing 10,010 images and 42,924 bounding boxes across seven extreme weather conditions: rain, snow, fog, haze/sand/dust, flooding, tornado, and wildfire. The dataset covers six traffic-object categories, including car, person, truck, motorcycle, bicycle, and bus. XWOD extends the weather taxonomy from one to seven conditions, and is the first to cover the emerging class of climate-amplified hazards, such as flooding, tornado, and wildfire. To evaluate the quality of our data, we train standard YOLO-family detectors on XWOD and test them zero-shot on external weather benchmarks, achieving mAP₅₀ scores of 63.00% on RTTS, 59.94% on DAWN, and 61.12% on WEDGE, compared with the corresponding published YOLO-based baselines of 40.37%, 32.75%, and 45.41%, respectively, representing relative improvements of 56%, 83%, and 35%. These cross-dataset results show that XWOD provides a strong source domain for learning weather-robust traffic perception. We release the dataset, splits, baseline weights, and reproducible evaluation code under a research-use license.

1 Introduction

In recent years, camera-based perception systems have been widely deployed in passenger vehicles, autonomous taxis, and delivery robots, but their reliability under extreme weather remains limited [36]. This gap is safety-critical: the five-year average data of U.S. Federal Highway Administration (FHWA) 2019–2023 attribute about 12% of crashes, 9% of traffic fatalities, and 11% of injuries to weather-related events [30]. In October 2024, the NHTSA Office of Defects Investigation opened a preliminary evaluation covering approximately 2.4 million Tesla vehicles after four Full Self-Driving crashes under reduced roadway visibility, including one pedestrian fatality [17]. Similar failures have also been observed in commercial robotaxi deployments in dense fog [27]. Recent robotaxi deployments further indicate that extreme weather remains a practical operational challenge. Waymo has temporarily paused or adjusted services during flash-flood conditions in San Francisco and San Antonio, and reports from Austin suggest that standing water can still affect robotaxi

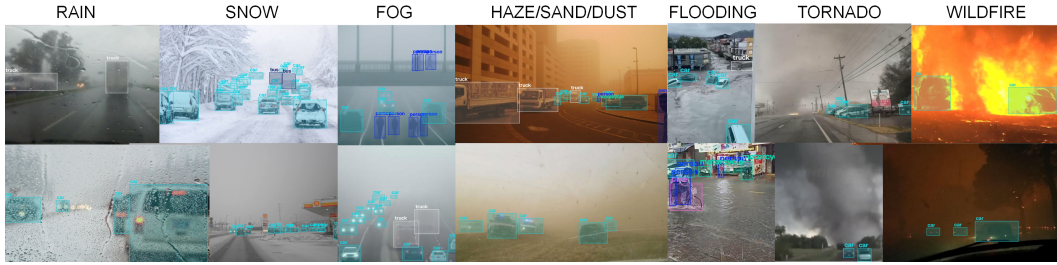


Figure 1: Representative samples of XWOD: The XWOD dataset provides a wide range of real-world extreme weather images with precise annotations, capturing rare, high-impact events such as floods, tornadoes, and wildfires to push robust computer vision boundaries.

operation on public roads [7, 12, 15]. These cases show that adverse-weather perception remains a major robustness bottleneck for real-world autonomy. Moreover, climate change is broadening the operational distribution that perception systems must handle, including wildfire smoke, flash flooding, urban inundation, and severe convective weather events [18].

Existing extreme-weather object detection benchmarks remain limited in four aspects, as summarized in Table 1. First, the scale is small: real-image datasets range from 1,000 images in DAWN [11] to 4,322 images in RTTS [13]. Second, the weather coverage is narrow. Most datasets focus on a single condition, such as haze in RTTS or fog in MAS, while multi-weather datasets such as ACDC and DAWN cover only four conditions. They do not include emerging climate-amplified hazards such as flooding, tornadoes, and wildfires. Third, existing datasets have strong geographic bias: RTTS is collected in China, MAS [24] in Zurich, and ACDC [26] mainly in Central Europe, which limits their ability to evaluate cross-region generalization to North American and Asian traffic environments. Fourth, data provenance is often constrained. Synthetic datasets such as WEDGE reduce collection cost, but they may inherit the biases of their generative pipelines, and prior work has shown that models trained only on synthetic data transfer imperfectly to real adverse-weather images [25].

In order to address these limitations, we created a new dataset called XWOD (eXtreme Weather Object Detection), containing 10,010 images and 42,924 object annotations. The sample images are shown in Figure 1. Our dataset is approximately $2.3\times$ larger than RTTS, $2.5\times$ larger than ACDC, and $10\times$ larger than DAWN. To our knowledge, XWOD is the first real-image object detection benchmark that includes tornado, flooding, and wildfire scenes. It is designed to evaluate object detection robustness under real-world weather distribution shifts, especially rare and climate-amplified hazards.

The main contributions of this work are summarized as follows:

- We introduce XWOD, the largest real-image traffic object detection benchmark for extreme weather, containing 10,010 images and 42,924 bounding boxes across seven weather types, six traffic categories, and four continents.
- We demonstrate strong zero-shot cross-dataset transfer. XWOD-trained detectors improve mAP_{50} from 40.37% to 63.00% on RTTS, from 32.75% to 59.94% on DAWN, and from 45.41% to 61.12% on WEDGE, corresponding to relative improvements of 56%, 83%, and 35%, respectively.
- We show that XWOD is a discriminative benchmark beyond dataset scaling. Performance is not determined solely by model size or architecture, since newer YOLO families and larger variants do not consistently outperform earlier or smaller models. This suggests that XWOD evaluates robustness to diverse weather-induced domain shifts rather than only measuring model scaling effects.

We release the dataset, splits, baseline weights, datasheet, and reproducible evaluation code under a research-use license on Kaggle¹.

¹<https://www.kaggle.com/datasets/kuantinglai/exwod>

2 Related Work

Extreme-weather driving datasets. *Foggy Cityscapes* [25] and *Foggy Zurich / MAS* [24] established the synthetic-vs-real-fog paradigm. RTTS [13] provides 4,322 real hazy images and is still the most-used real-haze detection testbed. ACDC [26] supplies 4,006 semantic-segmentation frames evenly divided across fog/night/rain/snow with clear-weather correspondences. DAWN [11] contains 1,000 web-sourced images across fog, snow, rain, and sandstorms. WEDGE [16] replaces collection with DALL-E generation, yielding 3,360 images across 16 labels, but images retain VLM-style hallucinations and copyright provenance questions. Multimodal large-scale sensor datasets include *Seeing Through Fog* [1], *CADC* [20], *Ithaca365* [6], *Boreas* [2], which focus on multimodal fusion and 3D perception rather than camera-based 2D detection. Those datasets are complementary but not comparable. BDD100K [35] includes weather tags but is dominated by clear-weather frames. XWOD is purely 2D camera detection and is the first dataset to cover climate-amplified hazards (flooding, tornado, wildfire).

Object detectors. Two-stage detectors [3, 22] remain common baselines in domain-adaptation studies. DETR and descendants [4, 37, 39, 40] and their real-time variants RT-DETR [38], D-FINE [19], and RF-DETR [23] push accuracy-latency frontiers. The YOLO family remains the most widely deployed in production driving stacks; recent releases include YOLOv7 [32], YOLOv8 [10], YOLOv9 [33], YOLOv10 [31], YOLOv11 [9], YOLOv12 [28], and YOLOv26 [29]. We benchmark YOLOv8, YOLOv11, and YOLOv26 since they bracket the current production landscape.

Weather-aware detection. Adaptive and restoration-coupled detectors explicitly train for weather correction: IA-YOLO [14] integrates differentiable image processing; TogetherNet [34] couples restoration and detection via dynamic feature enhancement; DENet [21] adds a Laplacian-pyramid enhancement front-end; DSNet [8] performs joint semantic learning. Domain-Adaptive Faster R-CNN [5] pioneered adversarial adaptation for object detection under foggy weather on Cityscapes.

3 The XWOD Dataset

3.1 Design Principles

Four principles guided XWOD’s design. (P1) **Real imagery only**: we avoided synthetic augmentation and generative imagery so that reported robustness reflects real-world distributions. (P2) **Coverage of climate-amplified hazards**: we expanded beyond the canonical rain/snow/fog triad to include haze/sand/dust, flooding, tornadoes, and wildfire conditions that are becoming more frequent and that lack prior benchmarks. (P3) **Geographic diversity**: images were sampled from Asia, North America, Europe, and the United States to limit regional texture bias. (P4) **Safety-relevant taxonomy**: we annotated the six traffic categories that dominate vehicle-person and vehicle-vehicle.

3.2 Data Collection

Images were sourced from (a) public traffic and weather-event photography archives, and (b) dashcam video frames donated by driving research partners. Furthermore, the XWOD dataset contains no personal or sensitive information. All images were sourced from public web platforms such as YouTube, adhering to their respective public usage policies. While the dataset includes the Person category as one of its six core traffic classes, these images represent pedestrians in public spaces and are not linked to any personally identifiable information (PII). Sensitive attributes such as gender, age, socioeconomic status, health data or political beliefs were not collected or annotated. (Appendix ??).

3.3 Annotation Protocol

We annotated the six traffic categories using axis-aligned bounding boxes. Following COCO-style protocols, our primary criterion was human recognizability: annotators labeled objects confidently identifiable despite weather degradation, while strictly excluding heavily obscured silhouettes to prevent noisy labels. A comprehensive visual guideline ensured high quality and consistency across all weather domains.

Table 1: Scale and provenance of real-image extreme-weather detection datasets. XWOD is the largest by image count and instance count, and the only one covering tornado, flooding, and wildfire.

Dataset	Year	Images	Instances	#Weather	Source
XWOD (ours)	2026	10,010	42,924	7	Asia, N. America, Europe, U.S.
RTTS [13]	2018	4,322	–	1	China
ACDC [26]	2021	4,006	–	4	Switzerland, central Europe
MAS / Foggy Zurich [24]	2018	3,808	–	1	Zurich, Switzerland
WEDGE [16]	2023	3,360	16,513	16	<i>Generative (DALL-E)</i>
DAWN [11]	2020	1,000	7,845	4	Web-sourced

Table 2: Per-weather image and instance counts, with mean boxes per image and mean relative box area. Rare-hazard classes (tornado, flooding, wildfire) contribute 72.7% of images and 67.8% of instances—the first time these conditions have been available at scale.

Weather	Images	Instances	Boxes/Img	Mean Rel. Area
Rain (heavy)	665	3,270	4.92	0.0244
Snow	1,203	5,599	4.65	0.0213
Fog	306	1,634	5.34	0.0333
Haze/Sand/Dust	560	3,321	5.93	0.0263
Flooding	5,151	21,734	4.22	0.0368
Tornado	1,164	4,962	4.26	0.0187
Wildfire	961	2,404	2.50	0.0586
Total	10,010	42,924	4.29	0.0316

3.4 Dataset Statistics

XWOD comprises 10,010 images and 42,924 labeled instances. Table 1 situates it among prior work. Tables 2 and 3 detail per-weather and per-class statistics. Average object count is 4.29 boxes per image; average relative box area of 0.0316, i.e., the benchmark is dominated by small-to-medium objects where weather degradation hurts most.

3.5 Splits

We release a fixed train / validation / test partition of 62%/15%/23% (6,206 / 1,744 / 2,060 images), stratified to preserve the per-weather and per-class distribution within each split. Split identifiers are shipped as plain-text index files. For XWOD-Gen (Section 4), we define an additional set of seven *leave-one-weather-out* splits used for cross-condition generalization.

4 Evaluation Protocols

XWOD defines two detection-side tracks plus a multimodal weather-understanding probe, each addressing a capability that standard mAP does not measure.

4.1 XWOD-Det: Standard Detection

Conventional mAP_{50} , mAP_{50-95} , precision and recall at IoU=0.5 in the fixed test split. Serves as the primary leaderboard and is comparable to COCO-style reporting. mAP breakdowns by weather are required for submissions.

4.2 XWOD-Gen: Leave-One-Weather-Out Generalization

For each weather $w \in \{1, \dots, 7\}$ we train in the other six and test in the holding condition. The reported metric is the *mean* and *worst* per-weather mAP across the seven runs.

$$\text{mAP}^{\text{Gen}} = \frac{1}{7} \sum_{w=1}^7 \text{mAP}_{w|\bar{w}}, \quad \text{mAP}_{\min}^{\text{Gen}} = \min_w \text{mAP}_{w|\bar{w}}. \quad (1)$$

Table 3: Per-weather class distribution (%). Distributions differ sharply by condition: flooding has the highest pedestrian and VRU share (46.49% non-vehicle), wildfire contains no motorcycles or bikes, and snow is car-dominated (85.25%).

Weather	Car (%)	Person (%)	Truck (%)	Motorcycle (%)	Bus (%)	Bike (%)
Rain	73.15	9.17	13.18	1.80	2.20	0.49
Snow	85.25	6.14	7.02	0.02	1.55	0.02
Fog	68.42	15.06	8.87	0.55	6.85	0.24
Haze/Sand/Dust	70.55	13.94	9.09	2.44	3.43	0.54
Flooding	37.56	32.37	15.17	7.23	0.77	6.89
Tornado	64.59	27.15	7.09	0.44	0.69	0.04
Wildfire	48.13	37.31	12.65	0.00	1.91	0.00
All	53.94	24.77	12.17	4.06	1.47	3.59

4.3 XWOD-LLM-WC: Weather Classification of LLMs

We define an image-only probes for vision-capable LLMs that use only labels already present in the released dataset, no extra annotation. We define a weather classification task, which aims to predict the weather class from {rain, snow, fog, haze/sand/dust, flooding, tornado, wildfire}. Metric: top-1 accuracy, macro-F1, and confusion matrix.

5 Baseline Experiments

5.1 Setup

Unless stated otherwise, detectors are trained for 100 epochs at input resolution 640×640 with the Ultralytics default SGD/AdamW schedule. We benchmark the YOLOv8, YOLOv11, and YOLOv26 families at the n/s/m/l/x scales. Experiments are conducted using a combination of a cloud computing environment, dynamically utilizing a pool of professional NVIDIA workstation GPUs (e.g., RTX A4500, and RTX 2000 to 6000 Ada Generation), and a local workstation equipped with an NVIDIA consumer-grade GPU (RTX 4060).

5.2 Optimization and Generalization

To address XWOD’s distributional shifts and long-tailed imbalances, we introduce a domain-specific optimization protocol for YOLOv11m. We use three training choices to improve robustness under extreme weather:

- **Robust optimization.** SGD with cosine annealing and 0.1 label smoothing is used to stabilize training under weather-induced texture degradation.
- **Mitigating long-tailed priors** The classification loss weight is increased to 1.5, with the learning rate set to 10^{-4} , to reduce inter-class confusion and improve minority-class learning.
- **Compositional and geometric augmentation.** Rectangular training is disabled, and Copy-Paste ($p = 0.2$), MixUp ($p = 0.1$), and random rotation within $\pm 10^\circ$ are applied to improve spatial diversity and rare-class exposure.

Training efficacy is validated in Figure 4. As shown in Fig. 4(a), it demonstrates superior transferability across synthetic (WEDGE), cross-weather (DAWN), and real-world (RTTS) domains, achieving 63.00% mAP₅₀ on RTTS (vs. 40.37%), 59.94% on DAWN (vs. 32.75%), and 61.12% on WEDGE (vs. 45.41%). Per-class analysis in Fig. 4(b) reveals a significant +16.28% overall gain, with dramatic improvements in rare categories: motorcycle (+25.01%), bus (+22.92%), and bike (+17.10%). These results confirm our optimizations effectively enable learning weather-invariant representations that generalize across unseen domains.

5.3 YOLO Family Comparison

Table 4 reports detection performance across the three architecture families and five scales. Three observations: (1) the *medium* variant is Pareto-best on XWOD for all three families, contrary to the

Table 4: YOLO family benchmark on XWOD-Det (test split) including loss metrics. Best per architecture in **bold**; overall best underlined. mAP, Precision, and Recall are in %; Loss values are absolute.

Family	Scale	mAP (%)		P / R (%)		Loss		
		mAP ₅₀	mAP ₅₀₋₉₅	Prec.	Rec.	Box	Cls	DFL
YOLOv8	n	49.24	28.74	63.59	46.79	0.9470	0.5195	0.9642
	s	51.53	30.60	63.42	49.23	0.7872	0.4000	0.9099
	m	54.69	32.21	63.05	53.51	0.7538	0.3715	0.9390
	l	52.53	31.34	68.37	47.13	0.6877	0.3341	0.9292
	x	52.70	30.97	63.08	50.28	0.6795	0.3269	0.9274
YOLOv11	n	46.91	27.36	65.09	43.77	0.9345	0.5184	0.9562
	s	48.35	28.47	60.85	47.81	0.8129	0.4210	0.9208
	m	53.84	31.93	63.33	53.47	0.7642	0.3899	0.9253
	l	52.06	30.86	62.33	49.75	0.7615	0.3788	0.9511
	x	52.64	31.41	59.97	52.39	0.7430	0.3702	0.9556
YOLOv26	n	46.29	26.73	57.92	45.27	1.1891	0.6250	0.0048
	s	51.92	30.49	63.74	50.18	1.0087	0.4349	0.0039
	m	53.34	32.29	70.40	48.24	0.9066	0.3674	0.0035
	l	53.95	32.75	66.24	51.77	0.9070	0.3627	0.0035
	x	53.61	32.55	67.59	51.85	0.8717	0.3458	0.0035

COCO pattern where larger scales continue to win; we attribute this to the high intra-class texture variance under weather, which regularizes smaller models; (2) YOLOv26l achieves the best overall mAP₅₀₋₉₅ of 32.75%, with YOLOv8m close behind at 32.21%; (3) YOLOv26m/l distribution focal loss is two orders of magnitude lower than YOLOv8/v11 due to its anchor-free regression redesign.

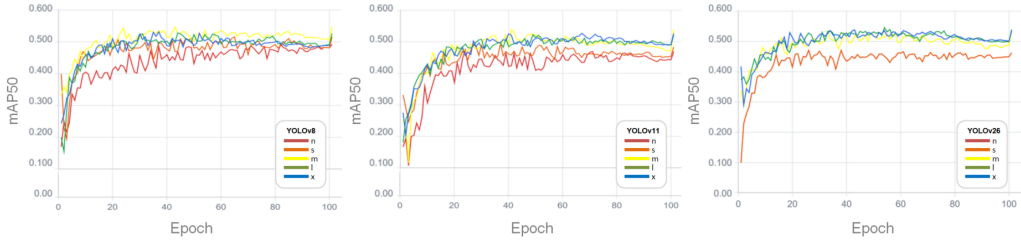


Figure 2: YOLO Family Training Curves.

Scaling and architecture alone are insufficient for extreme weather. Tab. 4 reveal that neither newer models nor larger scales consistently improve XWOD performance. YOLOv8 (49.24–54.69% mAP₅₀) often equals or surpasses YOLOv11 (46.91–53.84%) and YOLOv26 (46.29–53.95%), indicating no systematic gains from newer architectures.

Similarly, increasing scale yields marginal returns. Gaps between m, l, and x variants are typically 1–2% mAP₅₀, with medium models frequently outperforming largest counterparts. By breaking the "larger is better" assumption, XWOD reveals critical robustness limits. These marginal gains suggest that dataset diversity, rather than model scale, is the key to detector performance in extreme conditions.

5.4 Cross-Dataset Comparison

Table 5 compares XWOD with established extreme-weather benchmarks. Figure 3 shows the cross-dataset evaluation protocol. In contrast to benchmarks focused on specific conditions (e.g., RTTS haze or WEDGE synthetic imagery), XWOD captures a broader real-world spectrum, including climate-amplified hazards such as flooding, tornadoes, and wildfires.

The cross-dataset results indicate that XWOD can serve as an effective source domain for weather-robust traffic-object detection. A detector trained only on XWOD achieves 61.12% mAP₅₀ on WEDGE, 59.94% on DAWN, and 63.00% on RTTS, compared with the corresponding published

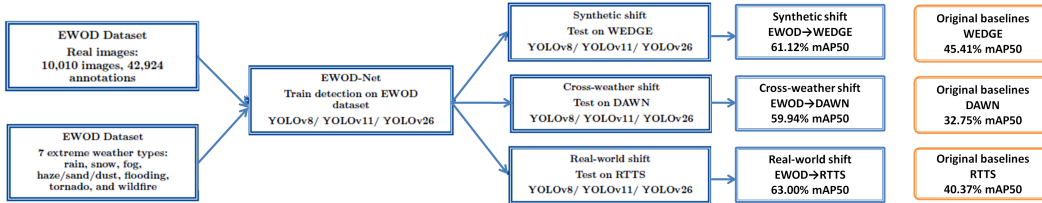


Figure 3: Evaluation Protocol of XWOD for weather-aware domain adaptation.

baselines of 45.41%, 32.75%, and 40.37%, respectively. These results correspond to relative improvements of 34.6%, 83.0%, and 56.1%. Since the published baselines differ in model architecture, training data, and evaluation protocol, these comparisons should be interpreted as evidence of XWOD’s transfer utility rather than as a controlled detector-level comparison.

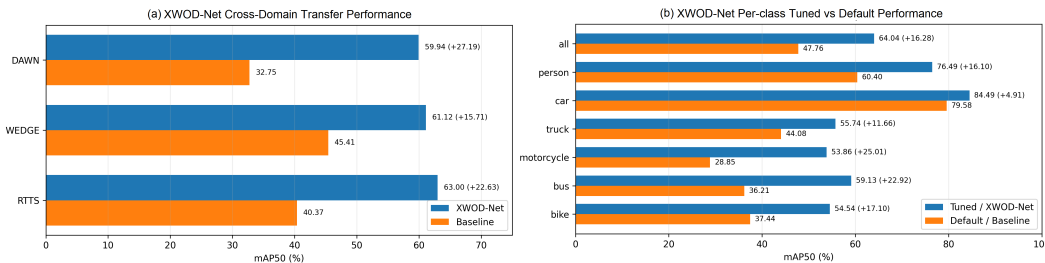


Figure 4: (a) YOLOv8m demonstrates strong generalization across synthetic (WEDGE), cross-weather (DAWN), and real-world (RTTS) domains, significantly outperforming native baselines. (b) YOLOv11m optimization protocol yields a +16.28% overall mAP₅₀ gain, with substantial improvements observed in rare categories such as motorcycle (+25.01%) and bus (+22.92%).

Table 6 further situates XWOD among related adverse-weather datasets. XWOD obtains 54.69% mAP₅₀ on its in-domain test set while covering seven weather conditions, including three rare climate-amplified hazards that are absent from prior real-image detection benchmarks. We therefore report XWOD primarily as a detection benchmark and treat segmentation-oriented datasets such as ACDC and MAS as complementary references rather than directly comparable quantitative baselines. Overall, the results suggest that real-world weather diversity improves cross-domain transfer and exposes failure modes that are not captured by narrower or synthetic benchmarks.

5.5 Per-Weather Breakdown

Table 7 reports YOLOv11m performance by weather, revealing a 51.12 pp gap between the best (tornado, 68.97% mAP₅₀) and worst (wildfire, 17.85%) conditions. Wildfire and fog dominate the error budget: wildfire degrades recall to 15.40%, the model finds only 1 in 6 objects, and fog halves recall relative to rain. These are the rare, safety-critical cases existing benchmarks never surfaced.

5.6 Weather Classification by LLMs

We also explore the image understanding ability of modern LLMs, and design a simple task that requests LLMs to classify the weather in our images. The task goal is that given a single street-level image, the LLM model must predict the dominant extreme weather condition as one of seven canonical labels: *rain, snow, fog, haze/sand/dust, flooding, tornado, wildfire*. Ground truth is read directly from the XWOD filename prefix (*heavy* → *rain*, *dust* → *haze/sand/dust*, etc.) and requires no additional annotation. The evaluation prompt is defined below. All vision-language models receive an identical zero-shot, single-turn prompt (no in-context examples, no chain of thought):

You are an expert in autonomous-driving scene understanding. Look at the image and classify the primary extreme weather condition as ONE of: rain | snow | fog | haze/sand/dust | flooding | tornado | wildfire. Reply with only the label, lowercase, no punctuation.

Table 5: Cross-domain evaluation against established baselines. Our XWOD models are trained on the XWOD dataset and tested zero-shot on unseen domains.

Category	Setting / Source	Model / Baseline	mAP ₅₀ (%)	Precision (%)	Recall (%)
In-domain (XWOD-Dataset)					
XWOD-Net	XWOD → XWOD	YOLOv8m	54.69	63.05	53.51
		YOLOv11m	53.87	63.33	53.47
		YOLOv26m	53.34	70.40	48.24
		YOLOv8l	52.53	68.37	47.13
		YOLOv11l	52.06	62.33	49.75
		YOLOv26l	53.95	66.24	51.77
Synthetic Domain Shift					
Baseline	WEDGE Original	Faster R-CNN	45.41	-	-
XWOD-Net	XWOD → WEDGE	YOLOv8m	61.12	66.23	55.98
		YOLOv11m	55.02	64.33	53.68
		YOLOv26m	53.94	71.83	49.00
		YOLOv8l	56.22	64.08	50.54
		YOLOv11l	55.29	64.16	53.95
		YOLOv26l	54.90	68.76	51.74
Cross-Weather Generalization					
Baseline	DAWN Original	Ensemble Det.	32.75	-	-
XWOD-Net	XWOD → DAWN	YOLOv8m	59.94	65.73	52.74
		YOLOv11m	55.17	61.81	52.18
		YOLOv26m	54.81	66.58	52.62
		YOLOv8l	55.28	66.37	53.95
		YOLOv11l	50.56	61.21	48.78
		YOLOv26l	56.99	72.08	52.08
Real-world Domain Adaptation					
Baseline	RTTS Original	Standard Det.	40.37	-	-
XWOD-Net	XWOD → RTTS	YOLOv8m	63.00	69.70	56.56
		YOLOv11m	54.57	69.65	50.67
		YOLOv26m	54.95	69.70	56.56
		YOLOv8l	60.31	64.53	55.09
		YOLOv11l	57.29	66.22	53.70
		YOLOv26l	56.74	67.95	53.07

Table 6: Cross-dataset comparison of best published detection results. “—” indicates the paper does not report that metric.

Dataset	Best Model	mAP (%) (All)	Best Per-Weather (%)	Notes
XWOD (ours)	YOLOv8m	54.69	62.93 (Tornado)	7 weather
	YOLOv11m	53.84	68.97 (Tornado)	7 weather
	YOLOv26l	53.95	66.01 (Tornado)	7 weather
RTTS [13]	—	40.37	—	1 weather
DAWN [11]	Ensemble	32.75	—	4 weather
WEDGE [16]	Faster R-CNN	22.78	—	16 labels, generative
	Fine-tuning	45.41	—	

The free-text reply is canonicalized via exact match, then a small keyword fallback (e.g. *foggy* → fog, *flood* → flooding, *fire* → wildfire) before scoring; unmatched outputs are kept as UNKNOWN.

Evaluation runs on the XWOD test split. To remove the long-tail imbalance from the metric, we sample a class-balanced probe of 100 images per class ($7 \times 100 = 700$ images total) using a fixed seed; images are re-shuffled before querying to avoid order effects. The whole probe is served to every model identically; per-image inputs are downsampled so the longest side is at most 1024 px and re-encoded as JPEG quality 90 to bound API token cost. Due to the limit of time and budget, we only select 4 latest LLM models for evaluation. The test results are shown in Table 8. All mainstream models have achieved high accuracy on the task. The top 1 and top 2 models are from Google Gemini family, followed by Claude Opus 4.7 and ChatGPT 5.5.

Table 7: Per-weather performance of YOLOv11m on XWOD-Det. Wildfire and fog are the clear failure modes. “Loss” columns from the final training epoch on each condition.

Weather	mAP ₅₀ (%)	mAP ₅₀₋₉₅ (%)	Prec. (%)	Rec. (%)	Box (loss)	Cls (loss)	DFL (loss)
Rain	60.49	37.70	61.74	61.87	0.699	0.406	0.938
Snow	38.46	25.93	69.79	32.19	0.534	0.314	0.810
Fog	23.45	11.97	66.08	21.92	0.976	0.564	1.168
Haze/Sand/Dust	29.86	9.95	38.83	35.10	0.650	0.390	0.888
Flooding	42.86	26.36	53.15	43.73	0.740	0.375	0.919
Tornado	68.97	43.47	75.38	57.70	0.771	0.415	0.905
Wildfire	17.85	12.18	60.57	15.42	0.409	0.279	0.845

Table 8: Weather classification performance of commercial LLMs.

Provider	Model Name	Accuracy	Macro F1
Google	gemini-3.1-pro-preview	0.7571	0.7585
Google	gemini-3.1-flash-lite-preview	0.7500	0.7500
Anthropic	claude-opus-4-7	0.7471	0.7446
OpenAI	gpt-5.5	0.7186	0.7221

6 Discussion

Wildfire and fog are open problems. XWOD detectors that score above 54.69% mAP₅₀ overall fall below 17.85% on wildfire and 23.45% on fog. The two conditions share the *contrast-suppression* failure mode: both collapse object-background color gradients and reduce mid-frequency texture, rendering anchor-based heads brittle. This motivates restoration-coupled detectors (IA-YOLO, TogetherNet, DENet), transformer backbones (RT-DETR, D-FINE), and open-vocabulary detectors (YOLO-World, Grounding DINO) as natural next candidates on XWOD-Det and XWOD-Gen.

Class prior versus weather prior. Flooding contains 6.90% bike instances vs. 0.02–0.55% in every other condition; wildfire contains *zero* motorcycle or bike instances. These asymmetric priors make leave-one-weather-out generalization (XWOD-Gen) a stringent test: models must avoid overfitting the joint (class, weather) prior while still exploiting it where correct.

Real versus synthetic. XWOD’s real imagery enables direct comparison with WEDGE’s VLM-generated scenes. Cross-evaluation could quantify the “real-data premium.” We anticipate synthetic-trained detectors will transfer poorly to XWOD’s flooding and wildfire splits, where generative models produce plausible but statistically mismatched scenes.

7 Limitations

XWOD has four main limitations. First, it is a 2D camera-based object detection benchmark and does not include LiDAR or radar signals commonly used in production autonomous-driving stacks; multimodal weather datasets such as STF [1], CADK [20] and Ithaca365 [6] are therefore complementary. Second, XWOD provides annotations for six traffic categories rather than the 19 classes used in some driving benchmarks, and is not designed for semantic segmentation. Third, although XWOD covers four continents, the weather distribution is imbalanced: flooding accounts for 51.5% of the images due to the greater availability of public flood imagery. We therefore report per-weather results to avoid masking this imbalance with aggregate metrics. Finally, tornado samples are limited to post-event or near-event scenes in which the tornado is visible in the frame. Pre-tornado conditions are not included.

8 Conclusion

We introduce XWOD, the largest real-image traffic object-detection benchmark for extreme weather to date. XWOD covers seven weather conditions and is the first benchmark to include the climate-amplified hazards of flooding, tornadoes, and wildfires. In addition to standard mAP evaluation,

we define two detection protocols, including leave-one-weather-out generalization (XWOD-Gen), and a multimodal weather-understanding probe (XWOD-LLM-WC). Our main empirical result is that XWOD provides a strong source domain for transfer learning: detectors trained *only* on XWOD outperform the published baselines of each target dataset under zero-shot evaluation on RTTS (63.00% vs. 40.37%), DAWN (59.94% vs. 32.75%), and WEDGE (61.12% vs. 45.41%). In-domain evaluation further reveals a 51.12-percentage-point gap across weather conditions, with wildfire and fog remaining the most challenging cases. XWOD is released with a datasheet, evaluation protocols, baseline weights, and reproducible code.

References

- [1] Mario Bijelic, Tobias Gruber, Fahim Mannan, Florian Kraus, Werner Ritter, Klaus Dietmayer, and Felix Heide. Seeing through fog without seeing fog: Deep multimodal sensor fusion in unseen adverse weather. In *CVPR*, 2020.
- [2] Keenan Burnett, David J. Yoon, Yuchen Wu, et al. Boreas: A multi-season autonomous driving dataset. *International Journal of Robotics Research*, 42(1–2):33–42, 2023.
- [3] Zhaowei Cai and Nuno Vasconcelos. Cascade R-CNN: Delving into high quality object detection. In *CVPR*, 2018.
- [4] Nicolas Carion, Francisco Massa, Gabriel Synnaeve, Nicolas Usunier, Alexander Kirillov, and Sergey Zagoruyko. End-to-end object detection with transformers. In *ECCV*, 2020.
- [5] Yuhua Chen, Wen Li, Christos Sakaridis, Dengxin Dai, and Luc Van Gool. Domain adaptive Faster R-CNN for object detection in the wild. In *CVPR*, 2018.
- [6] Carlos A. Diaz-Ruiz, Youya Xia, Yurong You, et al. Ithaca365: Dataset and driving perception under repeated and challenging weather conditions. In *CVPR*, 2022.
- [7] Spencer Heath. Waymo temporarily pauses San Antonio operations after vehicle entered flooded road. www.ksat.com/news/local/2026/04/21/waymo-temporarily-pauses-san-antonio-operations-after-vehicle-entered-flooded-road/, April 2026. KSAT. Accessed: 2026-05-07.
- [8] Shih-Chia Huang, Trung-Hieu Le, and Da-Wei Jaw. DSNet: Joint semantic learning for object detection in inclement weather conditions. *IEEE Transactions on Pattern Analysis and Machine Intelligence*, 2020.
- [9] Glenn Jocher and Jing Qiu. Ultralytics YOLO11. docs.ultralytics.com/models/yolo11/, 2024.
- [10] Glenn Jocher, Ayush Chaurasia, and Jing Qiu. Ultralytics yolov8, 2023. URL docs.ultralytics.com/models/yolov8/.
- [11] Mourad A. Kenk and M. Hassaballah. DAWN: Vehicle detection in adverse weather nature dataset, 2020.
- [12] KTVU Staff. Waymo pauses San Francisco service amid severe weather. www.ktvu.com/news/waymo-pauses-san-francisco-service-amid-severe-weather, December 2025. KTVU FOX 2. Accessed: 2026-05-07.
- [13] Boyi Li, Wenqi Ren, Dengpan Fu, Dacheng Tao, Dan Feng, Wenjun Zeng, and Zhangyang Wang. Benchmarking single-image dehazing and beyond. *IEEE Transactions on Image Processing*, 28(1):492–505, 2019.
- [14] Wenyu Liu, Gang Ren, Runsheng Yu, Shi Guo, Jianke Zhu, and Lei Zhang. Image-adaptive YOLO for object detection in adverse weather conditions. In *AAAI*, 2022.
- [15] Ethan Love. Video shows Waymo vehicles stopping in flooded Riverside Drive roadway. www.kxan.com/news/local/austin/video-shows-waymo-vehicles-stopping-in-flooded-riverside-drive-roadway, April 2026. KXAN. Accessed: 2026-05-07.

- [16] Aboli Marathe, Deva Ramanan, Rahee Walambe, and Ketan Kotecha. WEDGE: A multi-weather autonomous driving dataset built from generative vision-language models. In *CVPRW*, 2023.
- [17] NHTSA Office of Defects Investigation. Preliminary evaluation pe24031: Tesla full self-driving reduced roadway visibility crashes. static.nhtsa.gov/odi/inv/2024/INOA-PE24031-23232.pdf, 2024.
- [18] NOAA NCEI. 2024: An active year of U.S. billion-dollar weather and climate disasters. www.climate.gov/news-features/blogs/beyond-data, 2025.
- [19] Yansong Peng et al. D-FINE: Redefine regression task of DETRs as fine-grained distribution refinement. In *ICLR*, 2025.
- [20] Matthew Pitropov, Danson Evan Garcia, Jason Rebello, Michael Smart, Christine Wang, Krzysztof Czarnecki, and Steven Waslander. Canadian adverse driving conditions dataset. *International Journal of Robotics Research*, 40(4–5):681–690, 2021.
- [21] Qingpao Qin, Kan Chang, Mengyuan Huang, and Guiling Li. DENet: Detection-driven enhancement network for object detection under adverse weather conditions. In *ACCV*, 2022.
- [22] Shaoqing Ren, Kaiming He, Ross Girshick, and Jian Sun. Faster R-CNN: Towards real-time object detection with region proposal networks. In *NeurIPS*, 2015.
- [23] Roboflow. RF-DETR: Neural architecture search for real-time detection transformers. In *ICLR*, 2026.
- [24] Christos Sakaridis, Dengxin Dai, Simon Hecker, and Luc Van Gool. Model adaptation with synthetic and real data for semantic dense foggy scene understanding. In *ECCV*, 2018.
- [25] Christos Sakaridis, Dengxin Dai, and Luc Van Gool. Semantic foggy scene understanding with synthetic data. *International Journal of Computer Vision*, 126(9):973–992, 2018.
- [26] Christos Sakaridis, Dengxin Dai, and Luc Van Gool. ACDC: The adverse conditions dataset with correspondences for semantic driving scene understanding. In *ICCV*, 2021.
- [27] Rachel Swan. Waymo says dense S.F. fog brought 5 vehicles to a halt on Balboa Terrace street. www.sfchronicle.com/bayarea/article/san-francisco-waymo-stopped-in-street-17890821.php, April 2023. San Francisco Chronicle. Accessed: 2026-05-07.
- [28] Yunjie Tian, Qixiang Ye, and David Doermann. YOLOv12: Attention-centric real-time object detectors. In *NeurIPS*, 2025.
- [29] Ultralytics. YOLO26: Nms-free real-time detection. docs.ultralytics.com/models/yolo26/, arXiv:2509.25164, arXiv:2510.09653, 2026.
- [30] U.S. Federal Highway Administration. How do weather events affect roads? *Office of Operations, FHWA*, 2024. ops.fhwa.dot.gov/weather/q1_roadimpact.htm, five-year averages 2019–2023.
- [31] Ao Wang, Hui Chen, Lihao Liu, Kai Chen, Zijia Lin, Jungong Han, and Guiguang Ding. YOLOv10: Real-time end-to-end object detection. In *NeurIPS*, 2024.
- [32] Chien-Yao Wang, Alexey Bochkovskiy, and Hong-Yuan Mark Liao. Yolov7: Trainable bag-of-freebies sets new state-of-the-art for real-time object detectors. *Proceedings of the IEEE/CVF Conference on Computer Vision and Pattern Recognition (CVPR)*, pages 7212–7221, 2023.
- [33] Chien-Yao Wang, I-Hau Yeh, and Hong-Yuan Mark Liao. YOLOv9: Learning what you want to learn using programmable gradient information. In *ECCV*, 2024.
- [34] Yongzhen Wang et al. TogetherNet: Bridging image restoration and object detection together via dynamic enhancement learning. *Computer Graphics Forum*, 41(7):465–476, 2022.

- [35] Fisher Yu, Haofeng Chen, Xin Wang, Wenqi Xian, Yingying Chen, Fangchen Liu, Vashisht Madhavan, and Trevor Darrell. BDD100K: A diverse driving dataset for heterogeneous multitask learning. In *CVPR*, 2020.
- [36] S. Zang, M. Ding, D. Smith, N. Tyler, T. Rakotoarivelo, and M. A. Kaafar. The impact of adverse weather conditions on autonomous vehicles: How rain, snow, fog, and hail affect the performance of a self-driving car. *IEEE Vehicular Technology Magazine*, 14(2):103–111, 2019. doi: 10.1109/MVT.2019.2895591. URL ieeexplore.ieee.org. Provides a unified review of weather effects on LiDAR, GPS, Camera, and Radar.
- [37] Hao Zhang, Feng Li, Shilong Liu, Lei Zhang, Hang Su, Jun Zhu, Lionel M. Ni, and Heung-Yeung Shum. DINO: DETR with improved denoising anchor boxes for end-to-end object detection. In *ICLR*, 2023.
- [38] Yian Zhao, Wenyu Lv, Shangliang Xu, Jinman Wei, Guanzhong Wang, Qingqing Dang, Yi Liu, and Jie Chen. DETRs beat YOLOs on real-time object detection. In *CVPR*, 2024.
- [39] Xizhou Zhu, Weijie Su, Lewei Lu, Bin Li, Xiaogang Wang, and Jifeng Dai. Deformable DETR: Deformable transformers for end-to-end object detection. In *ICLR*, 2021.
- [40] Zhuofan Zong, Guanglu Song, and Yu Liu. DETRs with collaborative hybrid assignments training. In *ICCV*, 2023.